Lithium plating detection via EIS and ICA

Master's Thesis in Sustainable Electric Power Engineering and Electromobility

JINGHAN HE

DEPARTMENT OF ELECTRICAL ENGINEERING

CHALMERS UNIVERSITY OF TECHNOLOGY
Gothenburg, Sweden 2024
www.chalmers.se

Master's thesis 2024

Lithium plating detection using EIS and ICA

JINGHAN HE

CHALMERS
UNIVERSITY OF TECHNOLOGY

Department of electrical engineering
Division of electric power engineering
Chalmers University of Technology
Gothenburg, Sweden 2024

Lithium plating detection using EIS and ICA
JINGHAN HE

Supervisor: Erik Benjaminsson, Volvo Cars
Examiner: Torbjörn Thiringer, Department of Electrical Engineering

Master's Thesis 2024
Department of Electrical Engineering
Division of Electric Power Engineering
Chalmers University of Technology
SE-412 96 Gothenburg
Telephone +46 31 772 1000

Typeset in LaTeX
Printed by Chalmers Reproservice
Gothenburg, Sweden 2024

Lithium plating detection using EIS and ICA
JINGHAN HE
Department of Electrical Engineering
Chalmers University of Technology

Abstract

The rapid development of Fast Charging (FC) technology has significantly impacted the automotive industry, which is often accompanied by aging phenomena. This report presents a method to explore one such phenomenon: lithium plating. This method can help avoid conditions that lead to lithium plating during operation, thereby extending battery life and promoting Battery Electric Vehicles (BEVs) as viable alternatives to Internal Combustion Engine (ICE) vehicles. This report focuses on aging mechanisms, particularly lithium plating, and proposes a detection method using Electrochemical Impedance Spectroscopy (EIS), Incremental Capacity Analysis (ICA) and pulse test. Through comparative analysis and commercial battery testing, it verifies the reliability of the proposed method in identifying lithium plating during aging, which is beneficial for battery performance management.
The result of this study is that both single-sine and multi-sine methods are equally effective in analyzing electrochemical systems. The voltage required to induce lithium plating varies across different materials, with the voltage limit of $LiNi_{0.6}Mn_{0.2}Co_{0.2}O_2$ (NMC622) being lower than that of $LiNi_{0.8}Mn_{0.1}Co_{0.1}O_2$(NMC811). Additionally, NMC811 exhibits higher initial resistance compared to NMC622, with more pronounced resistance fluctuations. Overcharging and discharging lead to lithium plating, as evidenced by the Nyquist plot shifting to the right in EIS, a decrease in peak intensity in ICA, increased resistance in pulse tests with cycling, and a gradual decrease in capacity retention.

Keywords: Lithium Plating, Sustainability, Aging Phenomena, Electrochemical Impedance Spectroscopy, Incremental Capacity Analysis.

Acknowledgements

I want to thank everyone who helped me during my research. First, my supervisor Erik Benjaminsson, for his support and guidance. Also, thanks to Athmane Boulaoued for his academic advice. Muhammad Jawad Bhatti from the Battery Lab did the commercial cell experiments, and his expertise was crucial. Finally, I thank my teammate, Maria Olavarria Borrego, for her cooperation and support. Thank you all for your help in completing this research.

Jinghan He, Gothenburg, May 28th, 2024

List of Acronyms

Below is the list of acronyms that have been used throughout this thesis listed in alphabetical order:

FC	Fast Charging
BEVs	Battery Electric Vehicles
ICE	Internal Combustion Engine
EIS	Electrochemical Impedance Spectroscopy
ICA	Incremental Capacity Analysis
LFP	Lithium Iron Phosphate
NMC	Lithium Nickel Manganese Cobalt Oxide
LTO	Lithium Titanate
SOC	State of Charge
SOH	State of Health
SEI	Solid Electrolyte Interphase
SPI	Solid Permeable Interphase
GEIS	Galvanostatic
PEIS	Potentiostatic
KK	Kramers-Kronig
IC	Incremental Capacity
RPT	Reference Performance Test

Contents

1

Introduction

1.1 Backgroud

In recent years, the rapid development of Fast Charging (FC) technology has brought about a revolutionary change in the automotive industry. FC often accompanies some aging phenomena, and this report explore one of these aging phenomena, lithium plating. Studying this phenomenon is beneficial for better understanding battery life, thus making Battery Electric Vehicles (BEVs) more favorable replacements for traditional Internal Combustion Engine (ICE) vehicles. With several countries committing to reduce the use of gasoline and diesel vehicles by 2030 and accelerating plans to replace ICE with BEVs, the electric vehicle industry faces unprecedented development opportunities[1]. Achieving a high charging rate has become a key technical threshold for realizing this goal[2]. Advances in FC technology not only alleviate range anxiety during long-distance travel but also enable ultra-fast charging within 15 minutes[3].

Since the commercialization of lithium batteries in 1991, research on lithium-ion batteries has deepened, making lithium batteries with their high energy density the ideal choice for supporting long-distance driving[4]. However, to meet the market demand for fast charging capabilities of batteries, the challenges of accelerated battery aging and the decline in battery capacity and power must be confronted [5]. To address these challenges, at the end of 2020, the European Commission implemented battery regulation laws aimed at specifying recycling requirements for the main materials of batteries. This measure helps to improve the efficiency of material utilization in batteries, further advancing the sustainable development of the electric vehicle industry[6].

The degradation mechanisms can be divided into aging occurring on the cathode and on the anode. Aging on the anode includes film formation, loss of active material, and other structural changes. This report focuses on lithium plating, which is a type of active material loss. Particularly under FC conditions, it can lead to an increase in resistance[7]. The accumulation of lithium ions on the anode surface, particularly under extreme conditions, can lead to the formation of lithium dendrites, which can penetrate the separator and cause internal short circuits, thus posing serious safety risks[8][9].

1.2 Purpose

The purpose of this report is to detect lithium plating in batteries. This report uses Electrochemical Impedance Spectroscopy (EIS) to measure the electrochemical impedance spectrum and Incremental Capacity Analysis (ICA) to test the capacity of coin cell[10]. For data processing, this report uses the traditional equivalent circuits to handle the data. Subsequently, this report compares the outcomes derived from these methodologies. Concurrently, this report conducts EIS tests on commercial batteries with different levels of fast charging to verify if the observed aging patterns align with those obtained from the coin cell, thus validating the previous findings. This report aims to address the challenge of accurately identifying lithium plating phenomena during battery aging, ultimately enhancing the understanding and management of battery performance degradation.

1.3 Sustainability

BEVs are widely regarded as a more energy-efficient and environmentally friendly mode of transportation. For example, in China, pure electric vehicles can reduce CO_2 emissions by 37 % in regions with a high proportion of coal-fired power generation and by 90% in regions with a high proportion of hydropower[11]. However, they're not completely free from pollution. The process of generating electricity can lead to environmental pollution, and the production, processing, and recycling of batteries may also have negative environmental impacts. Hence, enhancing the efficiency of battery usage and strengthening recycling requirements are crucial for reducing the overall environmental footprint[12].

1.4 Ethics

In this report, certain sensitive data have been held back to protect intellectual property and the privacy of collaborators. All disclosed information is ensured to be authentic and accurate, preventing any academic misconduct.

2

Theory

2.1 Lithium-ion Batteries(LIBs)

Lithium-ion batteries are popular because of high energy density, quick charging capabilities, and long lifespan. This technology is considered promising for energy storage and is increasingly being used in everyday life as a reliable power source[13].

The basic principle of LIBs involves the repeated migration of lithium ions between the cathode and anode to charge and discharge. The anode material is typically graphite, while the cathode materials commonly include Lithium Iron Phosphate (LFP), Lithium Nickel Manganese Cobalt (NMC), and Lithium Titanate (LTO).

2.1.1 Key States of LIBs

The stable operation and management of batteries require knowledge of the accurate state of charge (SOC) and state of health (SOH). These two parameters can be used to understand the battery's condition.

SOC is defined as the percentage of the current usable energy in the battery correlated to the current SOH of the battery cell. It can be used to predict future usage time based on the current SOC level, and to prevent overcharging or overdischarging. SOH is defined as the ratio of the battery's current energy storage capacity to its initial energy storage capacity. It can be used to predict the remaining lifespan of the battery[14].

2.2 Cell Aging Mechanism

Each cycle of lithium-ion battery usage causes irreversible degradation. Resistance increases and capacity decreases during repeated charge and discharge processes. Therefore, it is important to detect the cell aging mechanism to help mitigate battery aging[15]. Various factors contribute to cell degradation, which differs between the anode and cathode. This report focuses on the aging mechanisms at the anode, particularly on lithium plating, which also results in the loss of active material.

2.2.1 Anode Aging Mechanisms

At present, graphite is used as anode material, its aging mechanism is relatively simple and its development is relatively mature. The selection range of cathode materials is more diverse, and the aging mechanism is complex and highly flexible. Therefore, this report focuses on anode aging mechanism when graphite is used as anode[16]. For the anode, the aging mechanism can be divided into three types: film-formation and loss of active material, and other structural changes.

2.2.1.1 Solid Electrolyte Interphase

Solid Electrolyte Interphase (SEI) is a typical film formed when the solvent and salts in the electrolyte decompose on the surface of the negative electrode during the initial charge of the battery. This film on the negative electrode prevents further reactions between the negative electrode material and the electrolyte, thereby protecting the negative electrode material. However, during cycling, particles can crack, necessitating the formation of new SEI layers. As the SEI thickness gradually increases, resistance rises and battery capacity decreases, leading to battery aging.

2.2.1.2 Lithium Plating

Lithium plating is a typical loss of active material aging mechanism. During the charging of lithium-ion batteries, lithium ions from the cathode are intercalated into the graphite electrode, which leads to loss of active material and thus reduced capacity. This unevenness on the anode's surface increases the polarization effect of electrochemical reactions. This polarization effect makes the diffusion rate of lithium ions uneven on the electrode surface, thus increasing the overpotential during the charging process. This phenomenon also leads to more pathways for the transfer of electrons and ions, effectively creating parallel resistances, thereby reducing the overall resistance of the battery. In severe cases, a lot of lithium can gather inside the battery, causing high voltage in certain spots. This might lead to a short circuit inside the battery. Furthermore, the formation of lithium plating exacerbates the issues associated with the SEI. Once the lithium plating penetrates the SEI membrane, the SEI might keep forming on the lithium plating, making the lithium plating issue worse and creating a bad cycle. Therefore, dealing with lithium plating is a big challenge for making batteries work better and safer[17][18].

2.2.1.3 Other Structural Changes

The structure of the anode material is an additional factor contributing to battery degradation. During lithium ion intercalation and de-intercalation, some crack formation in particles occurs, leading to battery aging[17].

2.2.2 Cathode Aging Mechanisms

The aging of cathode and anode in batteries is similar. It also mainly happens in three ways: a film forms on the surface, active material lost, and other changes in the structure. Solid Permeable Interphase (SPI) is a film that forms on the cathode,

similar to the SEI on the anode, but with different materials. Additionally, there can be disruptions in the structure of the cathode, for example, particles splitting or cracking, which will lead to the capacity fade[17].

2.3 Test method

In this section, this report will introduce the principles of methods for monitoring batteries: EIS and ICA. Specifically, for EIS, this report will also explain the principles of single-sine and multi-sine impedance spectroscopy.

2.3.1 EIS

EIS is a highly sensitive electrochemical testing technique used to evaluate the electrochemical processes and performance inside lithium-ion batteries. EIS is a non-destructive technique that applies a small perturbation, such as current or voltage, typically in galvanostatic mode (GEIS) or potentiostatic mode (PEIS). It then measures the voltage in response to current or the current in response to voltage to obtain the impedance response. It can detect frequencies in the range of approximately 1 MHz to 1 mHz[19].

EIS is usually represented using Bode plots and Nyquist plots to describe the frequency response of the system. The Nyquist plot represents impedance at different frequencies, with the real part (Z_{re}) on the horizontal axis and the negative imaginary part ($-Z_{\mathrm{im}}$) usually on the vertical axis. The shape and size of the Nyquist plot can indicate impedance processes, including charge transfer reactions and diffusion-controlled processes, within the electrochemical system. Different batteries produce different Nyquist plots. Figure 2.1 shows an idealized Nyquist plot for a commercial lithium-ion battery at different frequencies[20].

Bode plots consist of two parts: the first part shows the relationship between frequency and impedance magnitude ($|Z|$), and the second part shows the relationship between frequency and phase angle (θ). In the first part, you can see how the system impedance changes with frequency, while in the second part, you can observe how the phase angle changes with frequency.

The measurement results of EIS must satisfy three types of relationships: causal relationship, linear relationship, and stable relationship. Kramers-Kronigis(KK) a commonly used validation method, and the KK relationship is based on the principle of causal relationship. EIS also requires the impedance response of the system to adhere to this physical causal relationship. This means that if the data conforms to the KK relationship, then these data are likely to be accurate and reliable. Conversely, if the data do not conform to the KK relationship, it may indicate problems in the measurement process or that the behavior of the system does not adhere to the linear assumption[21].

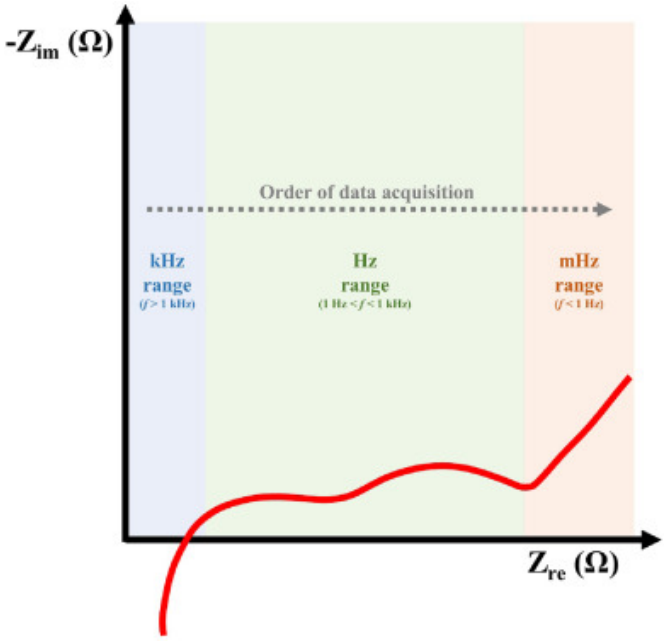

Figure 2.1: Nyquist plot[21]

2.3.1.1 Single-Sine Impedance Spectroscopy

Single-Sine Impedance Spectroscopy is a traditional type of EIS that follows all the basic principles of EIS. It involves applying a small-amplitude voltage or current excitation signal and obtaining the impedance response. Therefore, its principle is simpler because it only requires measuring one frequency of excitation signal, making it easier to implement and analyze.

2.3.1.2 Multi-Sine Impedance Spectroscopy

Multi-sine is also a type of EIS, where multiple sinusoidal signals of different frequencies are simultaneously used for excitation. This helps in obtaining more frequency response data in a shorter time, aiding in better understanding the dynamic behavior and characteristics of electrochemical systems. This relation can be represented as,

$$s(t) = \sum_{k=1}^{N} A_k \sin(2\pi f_k t + \phi_k) \tag{2.1}$$

In this equation, A_k represents the amplitude of each sinusoidal component, f_k represents the frequency, and ϕ_k represents the phase shift of each component. N is the number of sinusoidal components.

The multi-sine method can capture the dynamic response of the system more comprehensively, making it easier to meet the KK relation requirements. This method is more suitable for handling complex systems. In contrast, the single-sine method cannot capture all dynamic characteristics of the system during the measurement process, leading to deviations in the frequency-domain analysis[22].

2.3.2 Incremental Capacity Analysis(ICA)

ICA is commonly used to study the aging of batteries. By converting voltage changes caused by electrode phase transitions into an incremental capacity (IC) curve, the IC curve plots voltage on the horizontal axis and $\frac{dQ}{dV}$ (the rate of change of capacity with respect to voltage) on the vertical axis. The variations in the peak of the IC curve describe the phase transition characteristics during the intercalation and extraction processes and can reflect the degree of aging. The position, height, and area of the peaks in the IC curve are considered IC features, which are used to observe the decay of battery capacity more specifically.

To obtain more precise information, batteries are typically cycled at a constant low current. To achieve balanced battery parameters, the current is reduced to minimize the effects of resistance and diffusion.

2.3.3 Pulse test

The pulse test can determine the internal resistance of the battery by passing a current with a c-rate greater than 1, which leads to noticeable voltage changes. The voltage changes are measured, and according to Ohm's law, dividing the voltage change by the current change, thus obtaining the battery's internal resistance. This can be represented as,

$$R_{\text{internal}} = \frac{U_2 - U_1}{I_2 - I_1} \tag{2.2}$$

where U_1 and U_2 are the initial and final voltage values, and I_1 and I_2 are the initial and final current values.

2.3.4 Reference Performance Test (RPT)

RPT is a testing method used to evaluate battery performance by setting a reference and comparing other test results to it. The setup of the RPT can vary. In this report, the RPT setup includes capacity test, EIS measurement when SOC is at 10%, 30%, 50%, 70%, 90%, pulse test when SOC is at 30%, 50%, 70%, and ICA.

2.4 Data Processing Methods

In this section, this report will introduce the principles of methods for processing battery data: Equivalent Circuit Model. This method is used for analyzing EIS data in the frequency domain.

2.4.1 Equivalent Circuit Model

Traditionally, EIS usually uses the Equivalent Circuit Model to process data. Typically, resistors, capacitors, or constant phase elements are connected in series or

parallel based on experience to form an equivalent circuit, which simulates the actual circuit diagram. However, there is no perfect equivalent circuit diagram.

In lithium-ion batteries, Figure 2.2(a) is commonly used to represent LiB without lithium plating. Here, $Z_{\mathrm{dl,a}}$ and $R_{\mathrm{ct,a}}$ represent the anode interface, $Z_{\mathrm{dl,c}}$ and $R_{\mathrm{ct,c}}$ represent the cathode interface, and Z_{s} represents other influences from the electrolyte and SEI. This report adds an impedance Z_{w} after the parallel with $Z_{\mathrm{dl,a}}$ and $R_{\mathrm{ct,a}}$ to represent the diffusion process in the electrolyte.

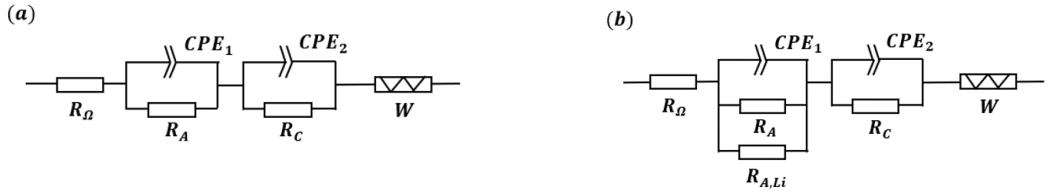

(a) (b)

Figure 2.2: Equivalent Circuit Model

As the battery undergoes continuous charge and discharge cycles, lithium plating occurs, leading to battery degradation. In consideration of this state, the equivalent circuit model will be modified by adding a resistor $R_{\mathrm{ct,Li}}$ in parallel with the anode. $R_{\mathrm{ct,Li}}$ represents the lithium plating reaction on the anode[23].

3

Methods

3.1 Case set up

This experiment is divided into two parts: coin cell and commercial cell. For the coin cell part, batteries are assembled using different nickel concentrations (NMC622 and NMC811) in three-electrode, with two samples for each material. Each battery is cycled at a rate of C/3 within the SOC range of 0-100%. One group is designated as a reference and cycled within the voltage range of 3V-4.25V. The other group undergoes overcharging with a voltage range of 3V-4.45V. All batteries undergo an EIS sweep every one week at SOC levels of 10%, 30%, 50%, 70%, and 90%, and an RPT every two weeks.

For the commercial cell part, after fast charging, EIS is conducted at SOC levels of 10%, 30%, 50%, 70%, and 90%. Finally, a comparison is made between the aging mechanisms observed in the coin cell and those in the commercial cell to determine if the findings from the coin cell can be verified in the commercial cell.

3.2 Experimental cells assembling

This experiment is conducted in a glove box to ensure that the batteries are in a dust-free, moisture-free, and oxygen-free environment. The experiment uses a PAT-cell, which is a type of coin cell. Figure 3.1 is a visualization of the PAT-cell. The steps for assembling the PAT-cell are as follows:

1. Place one-coated cathode material, anode material, insulation sleeve with lithium metal reference ring, and glass fiber separator, upper plunger, lower plunger, lower case, and upper case into the glovebox.
2. Put the cathode material on the separator, and block it with the lower plunger.
3. Place the separator and lithium metal reference ring, lower plunger, and cathode material into the lower case.
4. Add 100 μl of LiPF6 onto the separator.
5. Place the anode material onto the separator, ensuring the active material faces inside.

6. Stack the anode material with the upper plunger.
7. Place the upper case on the upper plunger and tighten it.

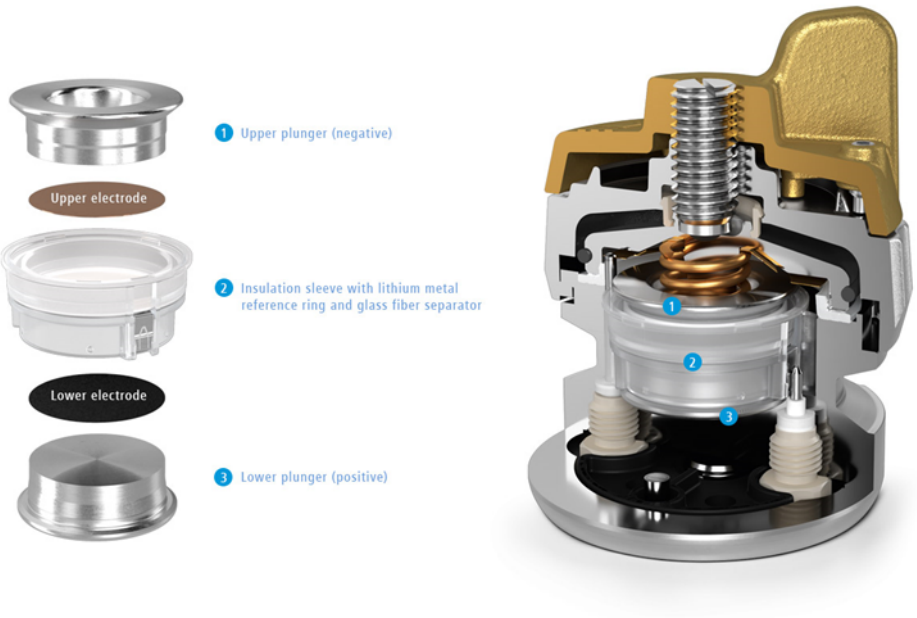

Figure 3.1: Structure of the PAT Cell[24]

3.3 Testing measurements of experimental

In this section, PAT-cells in coin cells will be cycled as an example. After cycling, PAT-cells will be tested using EIS measurements. Furthermore, commercial batteries after fast charging will also undergo EIS measurements. The results from coin cells and commercial batteries will be compared to observe patterns.

3.3.1 Coin cell

This report focuses on assembling coin cells, primarily because coin cells are easy to implement, have simple principles, and are easy to analyze. This approach can be helpful to discover aging mechanisms.

3.3.1.1 EIS hardware and software

The report will use three different laboratory testing instruments: BCS-810, VMP-3e, and PAT-Tester in coin cell. These instruments are to be utilized for experimentation, specifically for accommodating battery samples. The PAT-Tester is to be used in conjunction with Lab Event LT/100/40/5. The PAT-Tester will be placed inside the Lab Event LT/100/40/5, which serves as a thermal chamber. BCS-810 and VMP-3e are sourced from the same manufacturer and are controlled using the EC-LAB software. On the other hand, the PAT-Tester is controlled via EL-cell software. Despite the distinct software settings of these three instruments—Bio-logical

for BCS-810 and VMP-3e, and EL-cell for the PAT-Tester, their functionalities remain the same. Due to resource constraints, it is not possible to use instruments from the same brand. Therefore three different instruments and their corresponding software were selected for experimentation. Table 3.1-3.4 are the basic parameters of the four instruments:

Table 3.1: Characteristic of BCS-810

Voltage range	0V-10V
Current range	range 1A down to 0.1mA
EIS range	10kHz-10mHz

Table 3.2: Characteristic of VMP-3e

Acquisition time	200 μAs with EC-Lab
Current range	$\pm$ 10 μA to $\pm$ 1 A (6 ranges)
EIS capability	1 MHz to 10 μAHz
Compliance	20 V adjustable from $\pm$ 10 V between [-20 ; 20] V

Table 3.3: Characteristic of PAT-Tester

Control Voltage	-7 V to +7 V
Compliance Voltage	-8 V to 8 V (no load)
Current	$\pm$100 mA
Acquisition Time (Time Base)	1 ms
EIS range	10kHz-10mHz

Table 3.4: Characteristic of Lab Event LT/100/40/5

Minimum temperature	-40℃
Max temperature	100℃

3.3.1.2 Testing parameters

In this report, the protocol for testing is divided into three main sections: formation, reference performers test (RPT), and cycling.

In the formation step, a single cycle is conducted at a C-rate of C/20, followed by two cycles at a C-rate of C/10.

For the RPT step, two cycles are performed at a C-rate of C/3, followed by an additional cycle at C/3 to obtain capacity. Subsequently, the battery is charged to the cutoff voltage and discharged to various SOC levels: $90\%, 70\%, 50\%, 30\%$, and 10%. EIS measurements are taken at each of these SOC levels, while pulse tests are conducted at SOC $70\%, 50\%$, and 30% to determine internal resistance at each SOC level.

In the cycling step, the battery is cycled at a C-rate of C/3 within the SOC range of 1-100% for one week.

3.3.1.3 ICA measurements

In this report, an ICA measurement is carried out at a C-rate of C/25.

3.3.2 Commercial cell

This report also tests commercial cells that have only undergone EIS measurement, validating the patterns discovered from coin cells to see if the findings apply.

3.3.2.1 Parameters of Commercial Cells

The commercial cells are prismatic cell which have undergone fast charge.

3.3.2.2 EIS hardware and software

The report will use two different laboratory testing instruments: Climate Test Chambers and Gamry Instruments Reference 3000. The chamber will maintain the battery at 25° during EIS testing, while the Gamry instrument will be used for battery charging, discharging, and EIS testing. The Gamry instrument is controlled using the Gamry Framework software and data analysis is conducted using Gamry Echem Analyst. Table 3.5 and 3.6 are the basic parameters of the two instruments:

Table 3.5: Characteristic of Climate Test Chamber

Minimum temperature	-30℃
Max temperature	70℃

Table 3.6: Characteristic of PAT-Tester

Maximum Applied Potential	$\pm 35\,\mathrm{V}$
EIS range	$-10\,\mu\mathrm{Hz} - 1\,\mathrm{MHz}$

3.3.2.3 EIS parameters

In this report, commercial cell underwent EIS testing at SOC levels of 90%, 70%, 50%, 30%, and 10%. The initial SOC was set to 90%, and a constant current discharge of 30 Amps was applied. Voltage limit control was used as the cutoff condition for each SOC levels. The SOC levels of 70%, 50%, 30%, and 10% were used as voltage limits.

4

Results and Analysis

This chapter compares the results of the normally charged and discharged coin cells and those of cells with possible lithium plating induced by overcharge. Three testing methods which are EIS, ICA, and Pulse Test are used for analysis. Additionally, it validates the patterns by using the EIS of commercial cells that have already undergone fast charging and lithium plating.

4.1 Coin Cell

The testing is divided into two parts. One part serves as the reference group, which includes two sets of materials, NMC622 and NMC811, with normally charged and discharged cells, and each set contains two samples. The other part is the overcharge group, which also includes two sets of materials, NMC622 and NMC811, with overcharging to induce lithium plating, and each set contains two samples. This report analyzes only one sample from each material, while the other sample is kept as a backup. Cold temperatures and high C-rates are both reasons for lithium plating. This report chose overcharge because low temperatures increase resistance, which might lead to very high resistance. High C-rates might quickly reach the voltage limit during charging and discharging, potentially damaging the battery. In this report, 0RPT represents the first RPT after battery formation, 1RPT represents the RPT after two weeks of cycling, 2RPT represents the RPT after four weeks of cycling, 3RPT represents the RPT after six weeks of cycling. In the figure label, N6 represents the battery with NMC622 as the anode material, N8 represents the battery with NMC811 as the anode material, REF represents reference group, OVER represents overcharge group, CHAR represents charge, and DISC represents discharge.

4.1.1 Reference group

This section presents the results of EIS, ICA, and Pulse Tests conducted on the reference group of NMC622 and NMC811, and analyzes the findings.

4.1.1.1 EIS

Figure 4.1 compares the Nyquist plots of batteries on the reference group of NMC622 and NMC811 at SOC30% during 0RPT. It is found that the Nyquist plot of the

battery with NMC622 as the anode material has two semicircles, one representing the anode and the other representing the cathode. On the other hand, the Nyquist plot of the battery with NMC811 as the anode material has only one semicircle. This may be due to the properties of NMC622 and NMC811, which result in different time constants. The peaks for NMC811 are closer together, making it appear as though there is only one semicircle. This may be the reason why the Nyquist plot is different, but this is just a conjecture. To verify the results, a test must be added. The battery assembled with electrodes which will be manually cleaned and the battery assembled with electrodes provided by the supplier are tested simultaneously for EIS.

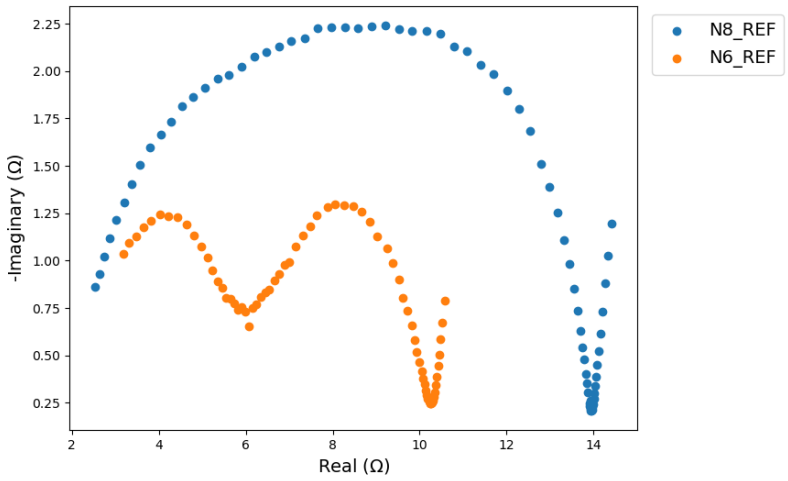

Figure 4.1: NMC622 and NMC811 Comparison at SOC30%

Figure 4.2 presents the Nyquist plots at 0RPT with NMC622 as the anode material. From the figure, it can be observed that as the SOC increases, the radius of the two semicircles also increase. This is consistent with the pattern indicated in Figure 4.3.

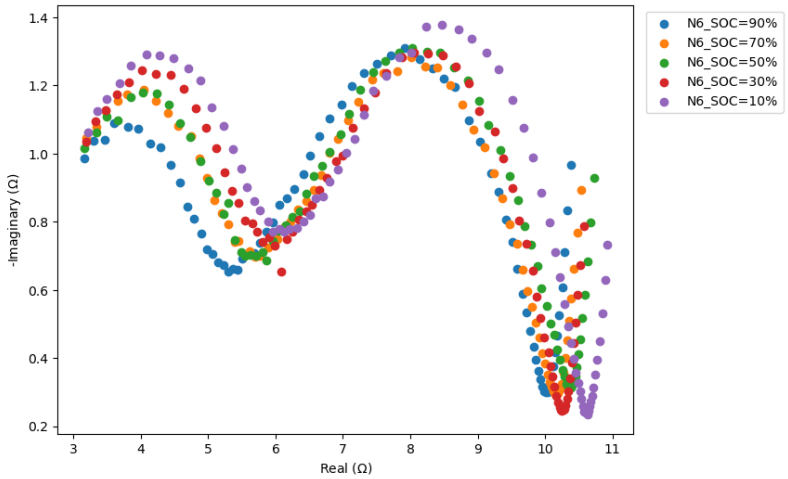

Figure 4.2: NMC622 Comparison at SOC10%,30%,50%,70% and 90%

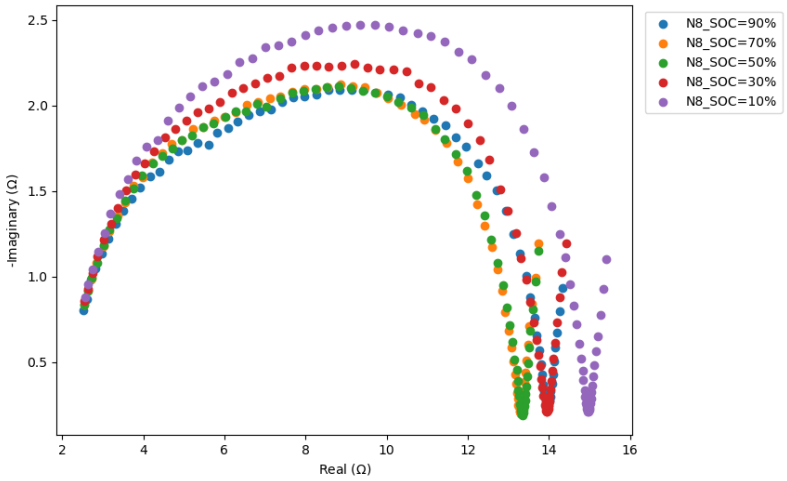

Figure 4.3: NMC811 comparison at SOC10%,30%,50%,70% and 90%

Figure 4.4 presents the Nyquist plots of the battery with NMC622 as the anode material at 0RPT, 1RPT, 2RPT and 3RPT. As the battery cycles, the starting points of each Nyquist curves move to the right, representing the increase in the battery's resistance. According to figure 4.5, batteries with NMC811 as the anode material also follow this pattern. Both graphs depict a fitting line simulated by the previously mentioned equivalent circuit model Figure 2.2.

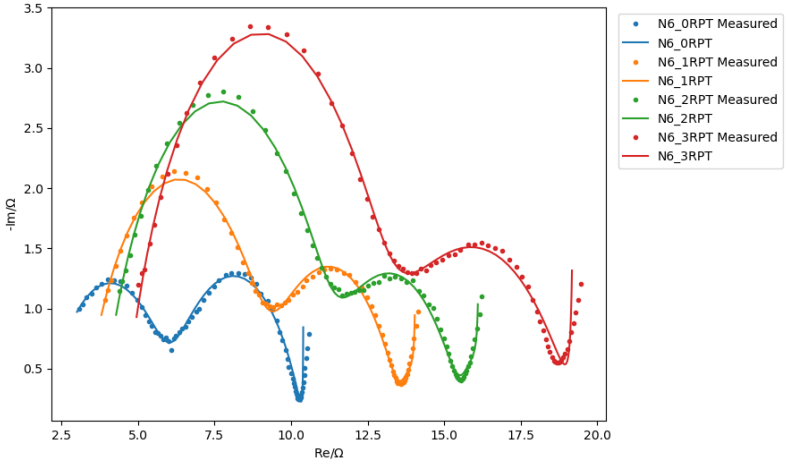

Figure 4.4: NMC622 at 0RPT, 1RPT, 2RPT, and 3RPT

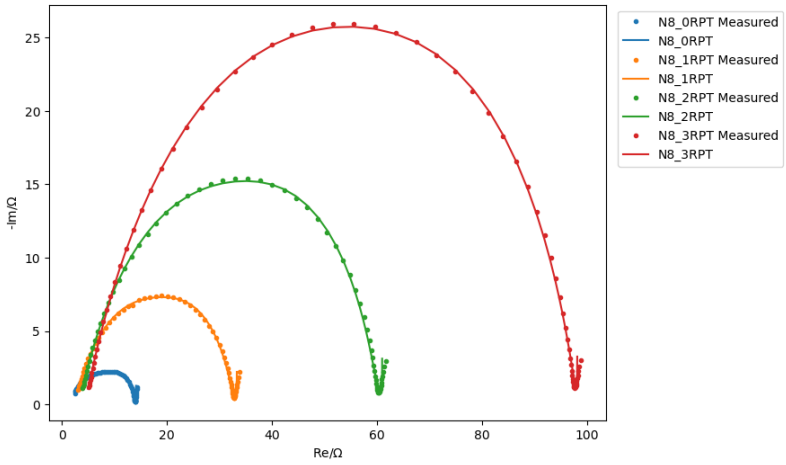

Figure 4.5: NMC811 at 0RPT, 1RPT, 2RPT, and 3RPT

Figure 4.6 presents when anode material with NMC622 at SOC10% using single sine signal and multi sine signal. The multi sine used in this report follows the same configuration as single sine mentioned in Section 3.3.1.1. The two lines almost overlap, which can be used to prove that these two measurement methods are equally effective in analyzing electrochemical systems. Because the other characteristics remain the same, with the only difference being the use of multi-sine or single-sine signal, the impedance characteristics captured by both methods are essentially consistent. As a result, the outcomes are similar.

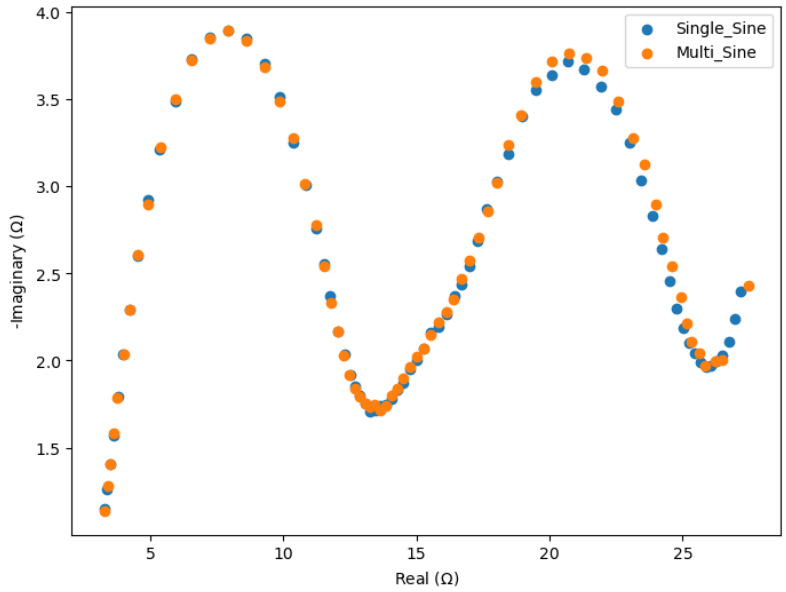

Figure 4.6: NMC622 at SOC10% with single and multi Sine Signal

4.1.1.2 Pulse Test

Figure 4.7 presents the Direct Current(DC) resistance obtained through pulse tests for batteries with NMC622 and NMC811 as the anode material at SOC 30%, 50%,

and 70%. It can be seen that the resistance of the NMC811-based battery is generally greater than that of the NMC622-based battery. This could be due to the higher nickel content of NMC811, which increases the battery's resistance. Additionally, the SOC level has little effect on the resistance of batteries with NMC622 and NMC811 as the anode material. At SOC 50%, the resistance is higher than at SOC 30% and SOC 70%. This is because the duration at SOC 50% is 30 seconds, and the longer pulse duration increases the polarization effect, leading to a higher measured resistance, which is longer than the 10 seconds at SOC 70% and SOC 30%.

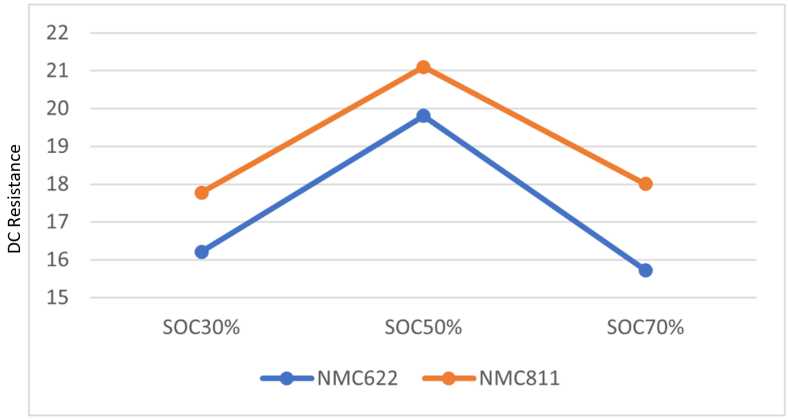

Figure 4.7: DC Resistance at 1.5CC Charge and Discharge: SOC 70% (T=10s), SOC 50% (T=30s), SOC 30% (T=10s)

Figure 4.8 shows the DC resistance of batteries with NMC622 and NMC811 as the anode material at 0RPT, 1RPT, and 2RPT, the Y-axis represents the growth rate of resistance, with the resistance value of all RPT0 considered as 1. As the battery cycles, the resistance of both NMC622 and NMC811 increases, but the increase in resistance for NMC811 is bigger than that for NMC622. This may be because NMC811 is less stable, resulting in bigger nickel content of it. There is no RPT3 point on the figure because when the pulse is performed during testing, as the resistance increases, the battery voltage reaches the limit voltage, so there is no valid pulse test.

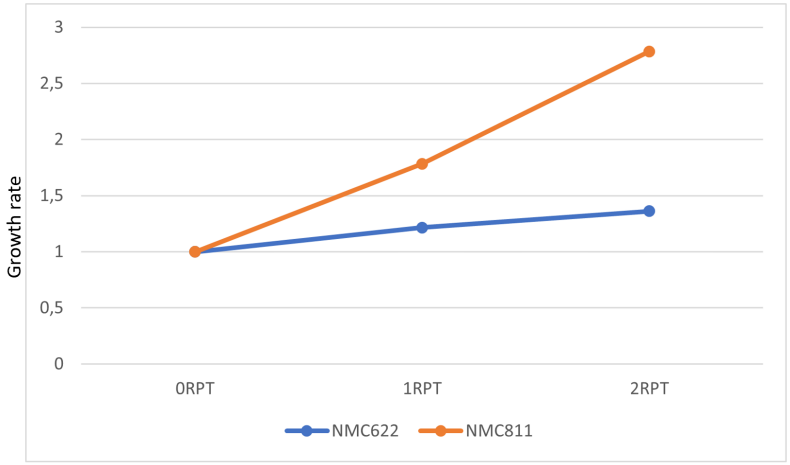

Figure 4.8: Growth Rate of DC Resistance for NMC622 and NMC811 at 0RPT, 1RPT, and 2RPT

4.1.1.3 ICA

Figure 4.9 shows the ICA of NMC622 and NMC811 at 0RPT. It can be seen that when the voltage is about 4.1V, NMC811 has a peak, which can help identify materials from figure.

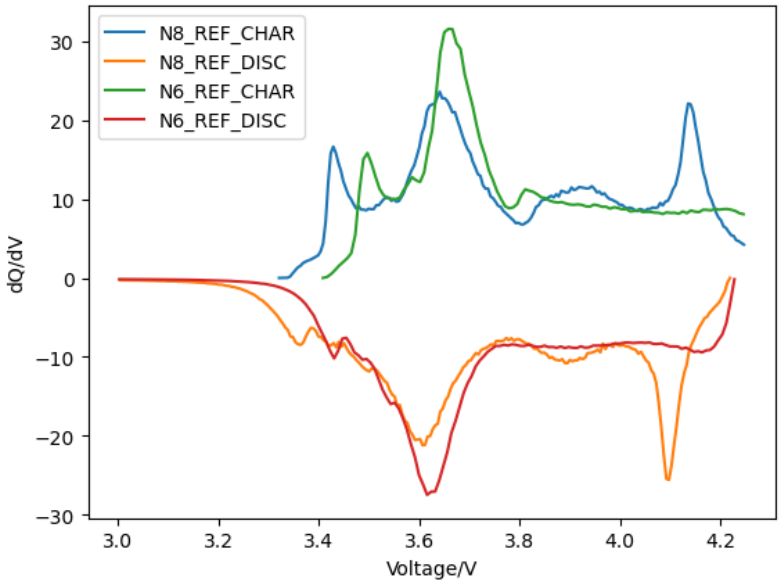

Figure 4.9: ICA Plot for NMC622 and NMC811 at C/25

Figure 4.10 shows the ICA of NMC622 at 0RPT, 1RPT, 2RPT, and 3RPT. As the battery cycles, the peak value at around 3.5V moves up slightly and shifts a bit to the right. The slight upward movement of the peak at 3.5V may due to measurement error, and more cycling is needed to see a clearer shift. The overall rightward shift is caused by the electrolyte drying out with cycling.

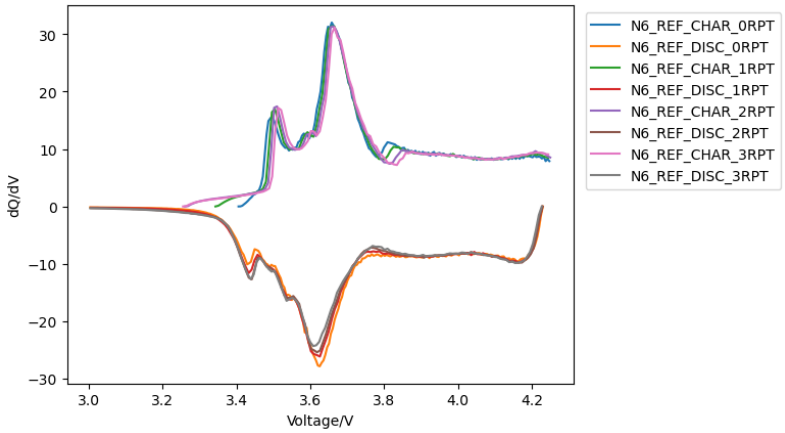

Figure 4.10: ICA Plot for NMC622 at 0RPT, 1RPT, 2RPT, and 3RPT at C/25

Figure 4.11 shows the ICA of NMC811 at 0RPT, 1RPT, 2RPT and 3RPT. As the battery cycles, it can be seen that all peaks are moving downwards, indicating a loss of active material with cycling. The movement is more obvious than NMC622. The reason for this noticeable change might be that NMC811 is more active.

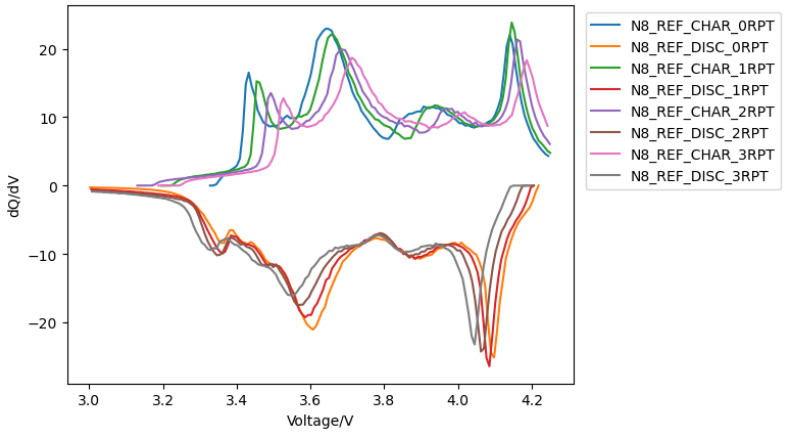

Figure 4.11: ICA plot for NMC811 at 0RPT, 1RPT, 2RPT and 3RPT at C/25

4.1.1.4 Capacity retention

Figure 4.12 shows the decreasing trend of NMC622 and NMC811 during common charge and discharge cycles. The decreasing trend of NMC811 is more significant due to the greater instability of its anode material. According to Figure 4.8, the resistance growth rate shows a significant increase. Interestingly, it is observed that when the resistance change is particularly pronounced, the capacity retention is notably lower.

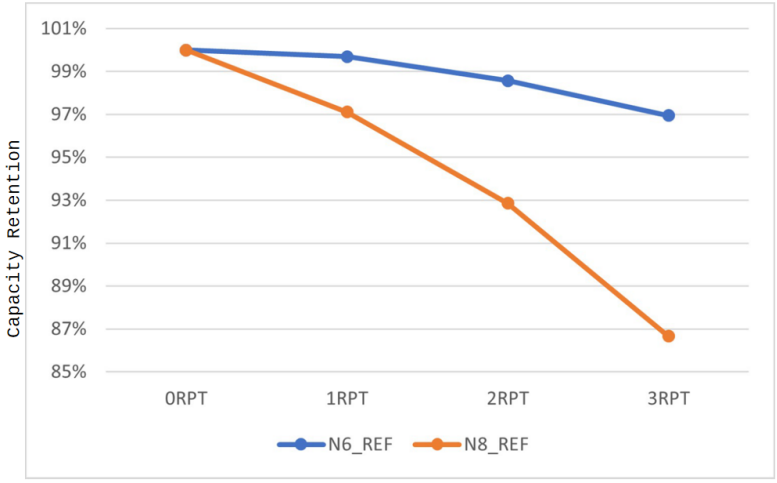

Figure 4.12: Capacity retention of NMC622 and NMC811

4.1.2 Overcharge group

This section shows data where cells are overcharged and discharged to force lithium plating to occur. It then compares these cells to ones that undergo regular charge and discharge cycles to analyze the impact of lithium plating on aging.

4.1.2.1 EIS

Figure 4.13 compares the Nyquist plots of the NMC622 reference group and the overcharge group at 0RPT, 1RPT, 2RPT and 3RPT. It demonstrates that with cycling, both cells shift to the right, indicating the increase of battery resistance.

Figure 4.14 is based on the equivalent circuit model and shows the NMC622 reference and overcharge groups: anode and ohmic resistance. The Y-axis represents the growth rate of resistance, with the resistance value of all RPT0 considered as 1. This figure indicates that the anode and ohmic Resistance all increase with cycling. Comparing the blue and grey lines, the anode resistance in the overcharge group increases more than that in the reference group. This could be due to two reasons: first, fitting errors in the data; second, initially setting the voltage limit low enough to cause the anode's voltage to drop below 0V, leading to lithium plating. However, figure 4.15 shows that the anode voltage gradually increases with cycling. This increase is because, as the battery ages, its resistance increases, making it easier to reach the cutoff voltage. As a result, there is not enough time for lithium plating to occur during charging. The aging effect is more significant than the lithium plating effect, causing the anode resistance in the overcharge group to increase more than in the reference group. Comparing the orange and yellow lines, the ohmic resistance in the reference group is greater than in the overcharge group. This might be because the initial resistance in the reference group was higher than in the overcharge group, or it could be due to fitting errors.

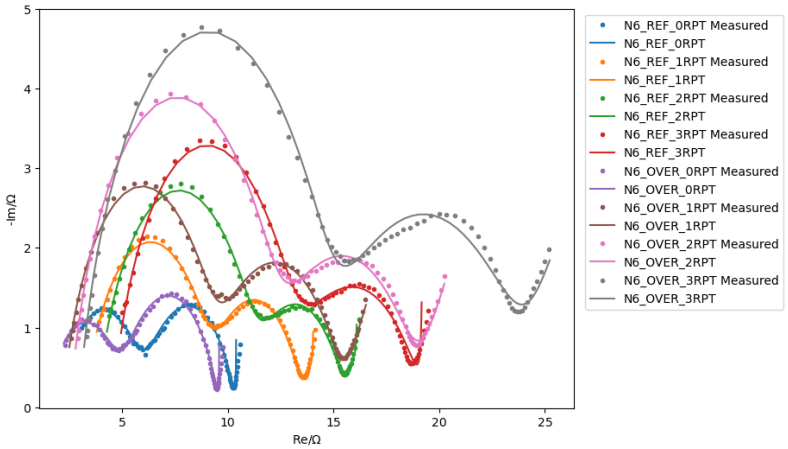

Figure 4.13: NMC622 at 0RPT, 1RPT, 2RPT and 3RPT, Normal vs. Overcharge

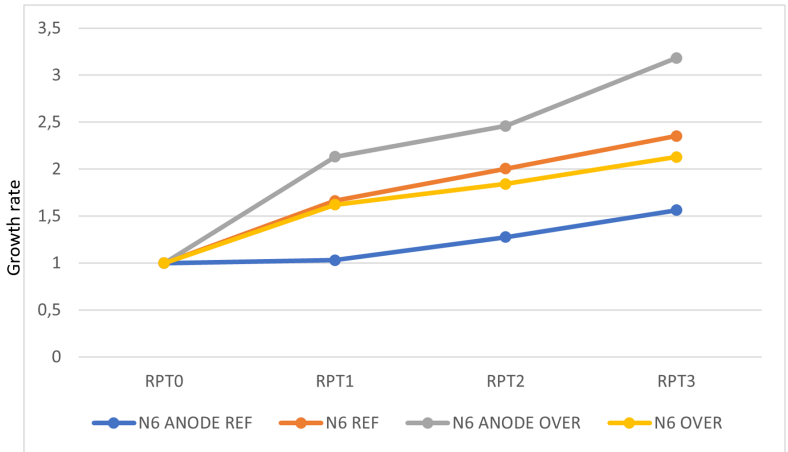

Figure 4.14: Comparative Growth Rate of Pulse Test Anode and Ohmic Resistance: NMC622 Reference vs. Overcharge Groups

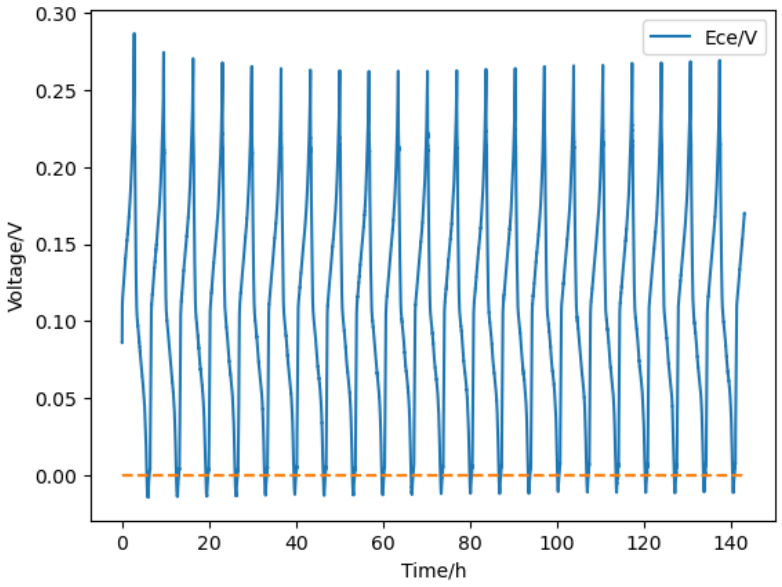

Figure 4.15: Anode Voltage of NMC622 in Overcharge Group During Cycling After 0RPT

Figure 4.16 compares the Nyquist plots of the NMC811 reference group and the overcharge group at 0RPT, 1RPT, 2RPT and 3RPT, similar to the anode material being NMC622, both cells shift to the right, indicating the increase of battery resistance. It is surprised that at 2RPT and 3RPT, the charge transfer resistance in the overcharge group is unexpectedly lower than that in the reference groups.

Figure 4.17 is based on the equivalent circuit model and shows the NMC811 reference and overcharge groups: anode and ohmic resistance. The Y-axis represents the growth rate of resistance, with the resistance value of all RPT0 considered as 1. The anode resistance in the reference group is higher than the overcharge group at 1RPT but lower at 2RPT, showing no consistent trend. This might be due to fitting issues. Figure 4.18 shows the anode voltage of NMC811 after 0RPT, which follows a similar trend to NMC622. The anode voltage starts below 0V but gradually increases, and this increase is more pronounced in NMC811. This could be because NMC811 is less stable than NMC622, making its resistance grow more easily and reach the voltage limit sooner. Additionally, the voltage limit was set based on NMC622's voltage, but NMC811 should have a higher voltage limit to force lithium plating. Comparing the orange and yellow lines in Figure 4.17, the ohmic resistance in the reference group is similar to that in the overcharge group. This might be because NMC811 is not reaching the real voltage limit.

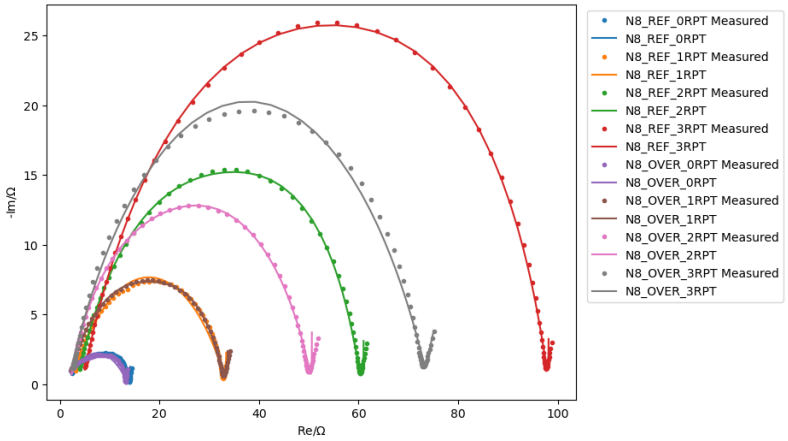

Figure 4.16: NMC811 at 0RPT, 1RPT, 2RPT and 3RPT, Normal vs. Overcharge

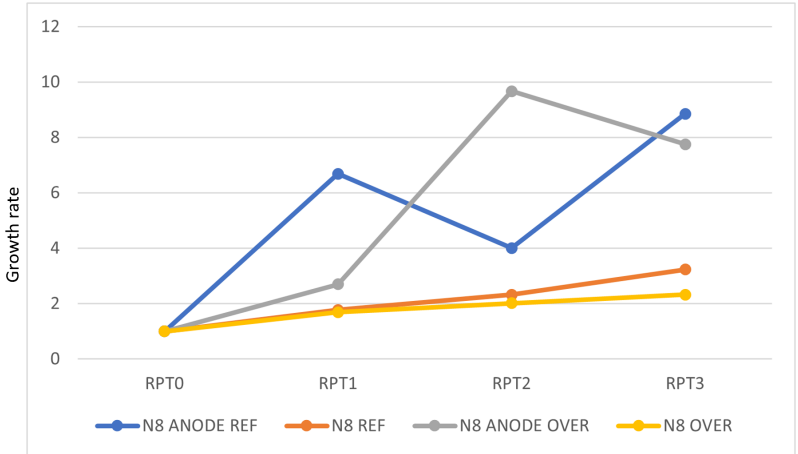

Figure 4.17: Comparative of NMC811 Reference and Overcharge Groups: Anode and Ohmic Resistance

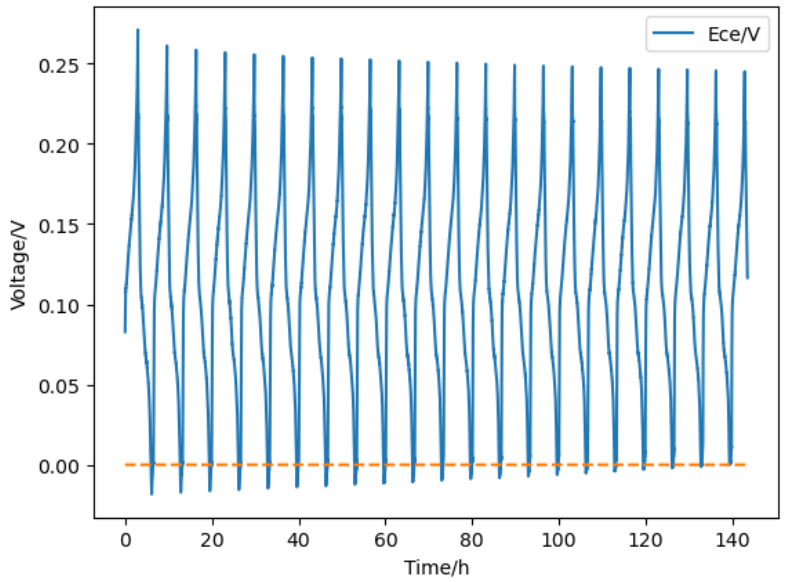

Figure 4.18: Anode Voltage of NMC811 in Overcharge Group During Cycling After 0RPT

4.1.2.2 Pulse Test

Figure 4.19 compares the DC resistance of the NMC622 reference group and the overcharge group at 0RPT, 1RPT, and 2RPT. The Y-axis represents the growth rate of resistance, with the resistance value of all RPT0 considered as 1. It can be seen that the resistance of both the reference group and the overcharge group will increase. However, the resistance of the overcharge group increases significantly more than that of the reference group. This is because overcharge will lead to the generation of lithium plating, which will accelerate the increase in resistance.

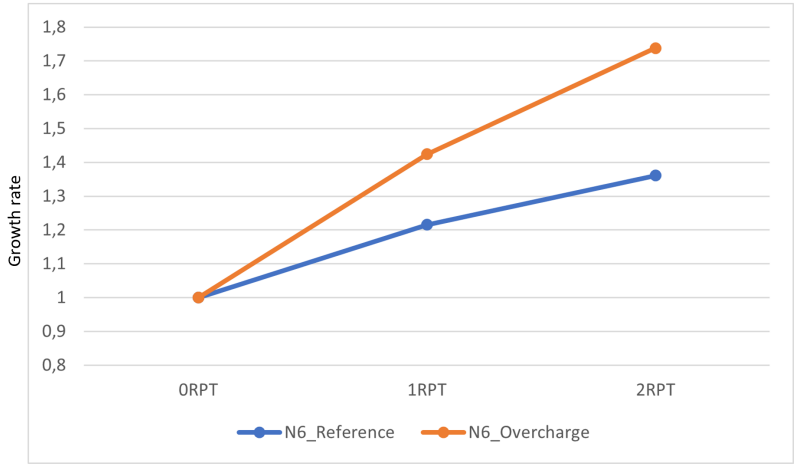

Figure 4.19: Growth Rate of DC Resistance of NMC622 at 0RPT, 1RPT, and 2RPT

Figure 4.20 compares the DC resistance of the NMC811 reference group and the

overcharge group at 0RPT, 1RPT, and 2RPT. It can be seen that the resistance R0 of both the reference group and the overcharge group will increase, but the change in resistance is not significant for either group. This might be because, as mentioned before, there is no clear difference between the reference group and the overcharge group in NMC811, and the effect of lithium plating is not obvious.

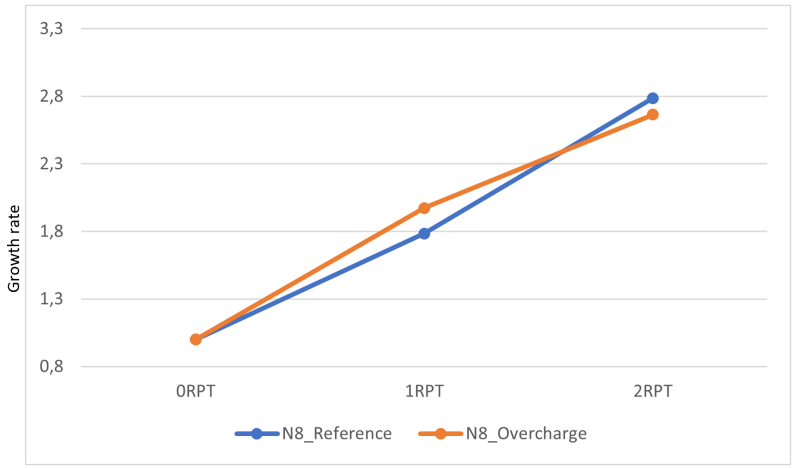

Figure 4.20: Growth Rate of DC Resistance of NMC811 at 0RPT, 1RPT, and 2RPT

4.1.2.3 ICA

Figure 4.21 shows the ICA plot of the NMC622 reference group and the overcharge group at 3RPT. It can be observed that the peak intensity in the 3.7V reference group is higher than in the overcharge group. This proves that the peak intensity in the overcharge group decreased more than in the reference group, indicating the occurrence of lithium plating in the overcharge group.

Figure 4.22 shows the ICA plot for the NMC622 cathode voltage at 3RPT. It seems that the peak intensity does not change significantly, but there is an overall rightward shift. This could be because the phase change in the electrode material requires a higher voltage. Figure 4.23 shows the ICA plot for the NMC622 anode voltage at 3RPT. It seems that the peak intensity near 0.1V for the overcharge group is lower than the reference group. This is because the overcharge group lost more active material than the reference group as cycling continued.

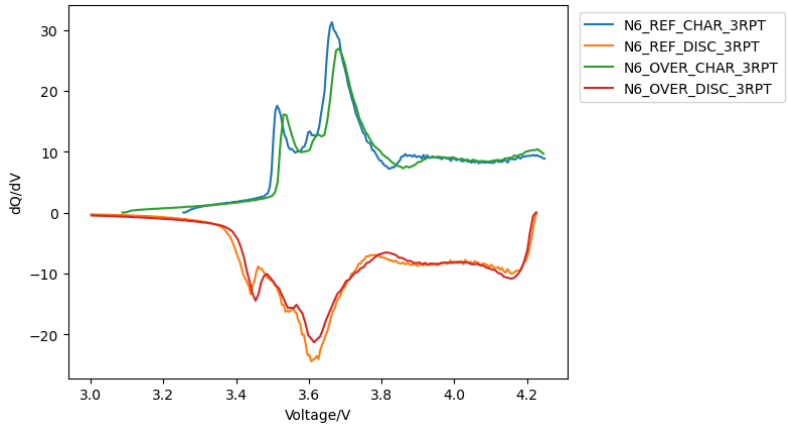

Figure 4.21: ICA plot for NMC622 at 0RPT, 1RPT, 2RPT and 3RPT at C/25, Normal vs. Overcharge

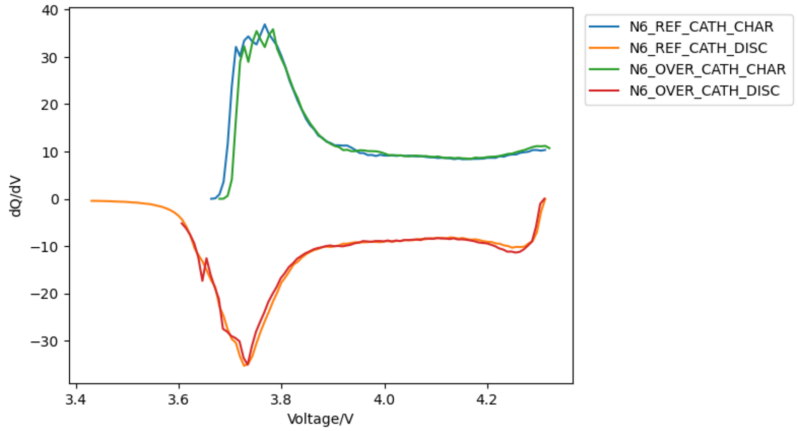

Figure 4.22: ICA plot for NMC622 cathode volage at 3RPT at C/25

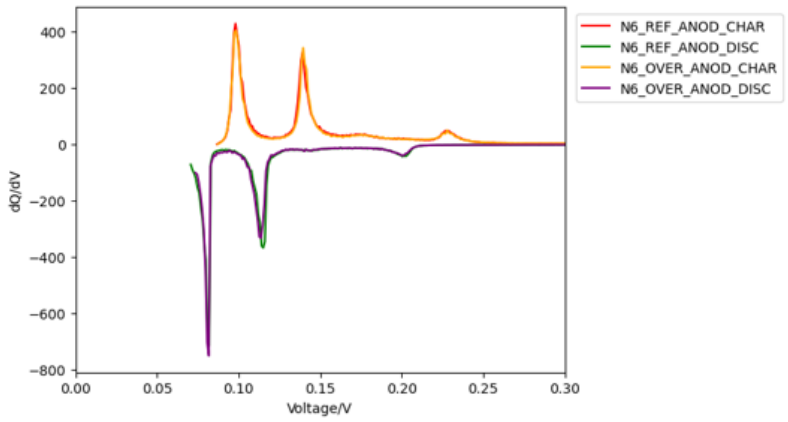

Figure 4.23: ICA plot for NMC622 anode voltage at 3RPT at C/25

Figure 4.24 shows the ICA plot of the NMC811 reference group and the overcharge group at 3RPT. It can be seen that the peak intensity in the reference group shifts

to the right compared to the overcharge group. This might be due to a lack of electrolyte.

Figure 4.25 shows the ICA plot for NMC811 cathode voltage at 3RPT. It can be seen that the changes in the cathode are significant with cycling. Figure 4.26 also shows the ICA plot for NMC811 anode voltage at 3RPT. It can be seen that the changes in the anode are not significant with cycling, further confirming that overcharge group of NMC811 may not have much lithium plating. However, observing that the first discharge point is very close to 0V represents a significant potential for lithium plating.

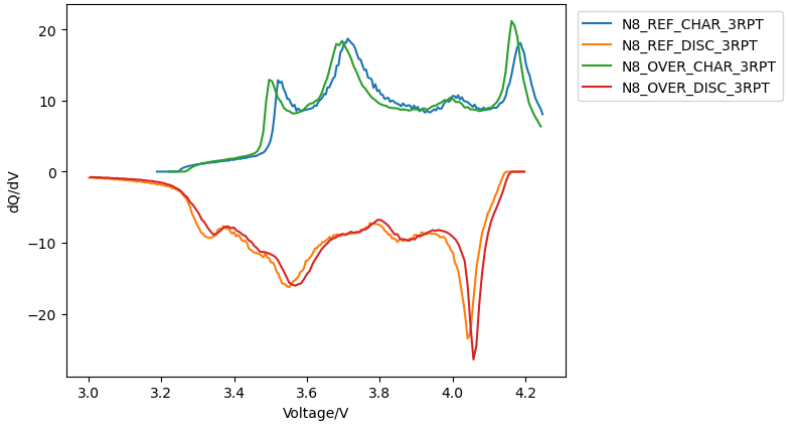

Figure 4.24: ICA plot for NMC811 at 3RPT at C/25, Normal vs. Overcharge

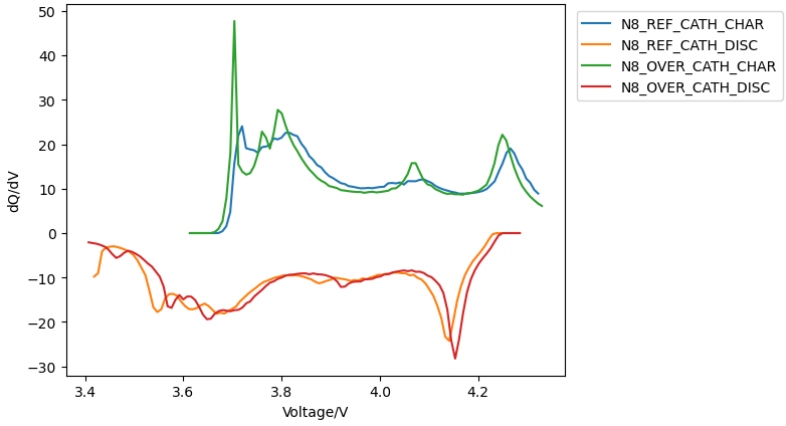

Figure 4.25: ICA plot for NMC811 cathode voltage at 3RPT at C/25

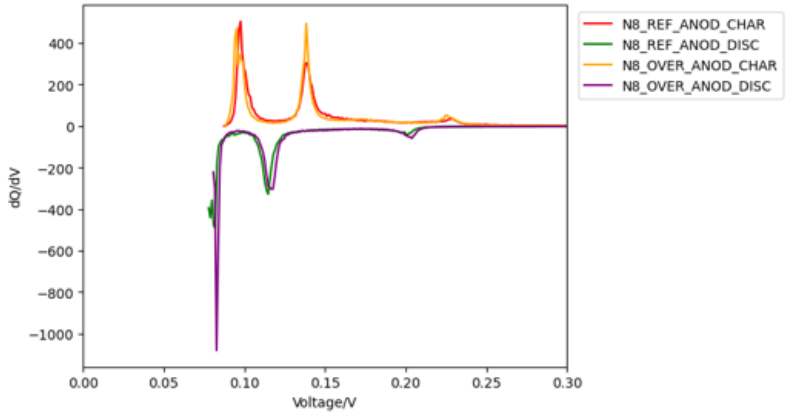

Figure 4.26: ICA plot for NMC811 anode voltage at 3RPT at C/25

4.1.2.4 Capacity retention

Figure 4.27 shows the capacity retention of the NMC622 reference group and the overcharge group at 0RPT, 1RPT, 2RPT and 3RPT. It can be observed that with cycling, the capacity of both the reference group and the overcharge group decreases. However, the capacity fade of the overcharge group is greater than that of the reference group. This is because the batteries in the overcharge group experienced lithium plating due to overcharging, leading to more capacity fade.

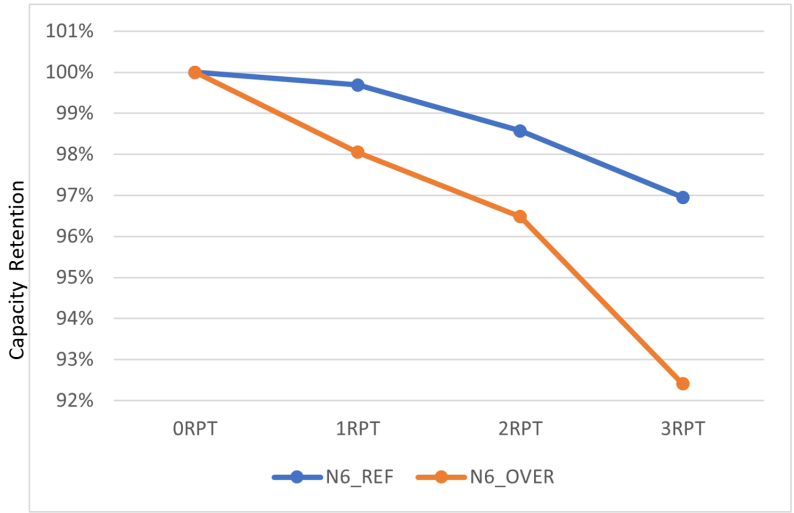

Figure 4.27: Capacity retention of the NMC622 at 0RPT, 1RPT, 2RPT and 3RPT

Figure 4.28 shows the capacity retention of the NMC811 reference group and the overcharge group at 0RPT, 1RPT, 2RPT and 3RPT. It can be seen that with cycling, the capacity of both the reference group and the overcharge group decreases. However, the capacity fade of the overcharge group is smaller than that of the reference group after 2RPT. This is because the voltage limit was set according to NMC622. As cycling continued, the resistance of NMC811 increased, making it

easier to reach the voltage limit. Therefore, there wasn't enough charge to cause lithium plating in NMC811.

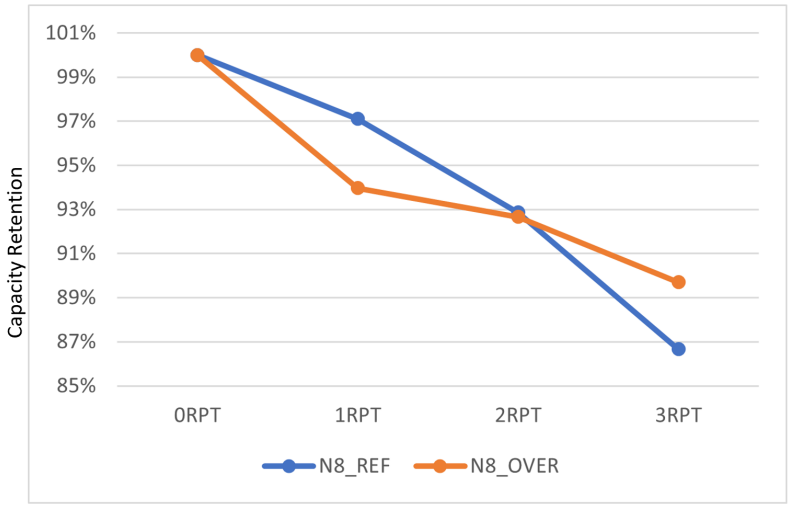

Figure 4.28: Capacity retention of the NMC811 at 0RPT, 1RPT, 2RPT and 3RPT

4.1.2.5 Battery Tear Down

This section displays the NMC622 and NMC811 after teardown. Figure 4.29 shows the NMC622 reference group. Since it was a tear down conducted at 100%SOC, lithium ions can be observed gathering on the anode, represented by the gold-colored areas. Figure 4.30 displays the overcharge group of NMC622. In this figure, there are some bubbles, which originate from the sealed plastic casing. Additionally, there are white spots stemming from the separator adhered to the anode. The gray sparkling dots seen on the figure represent lithium plating. Their limited presence may be attributed to the anode's voltage not dropping below 0V in the later stages of cycling.

Figure 4.31 shows the NMC811 reference group, figure 4.32 shows the NMC811 overcharge group. Both of these figure don't have any obvious shiny gray dots. This might be because it's easy to reach the voltage limit, which leads to not enough charging time, and thus, no lithium plating occurs.

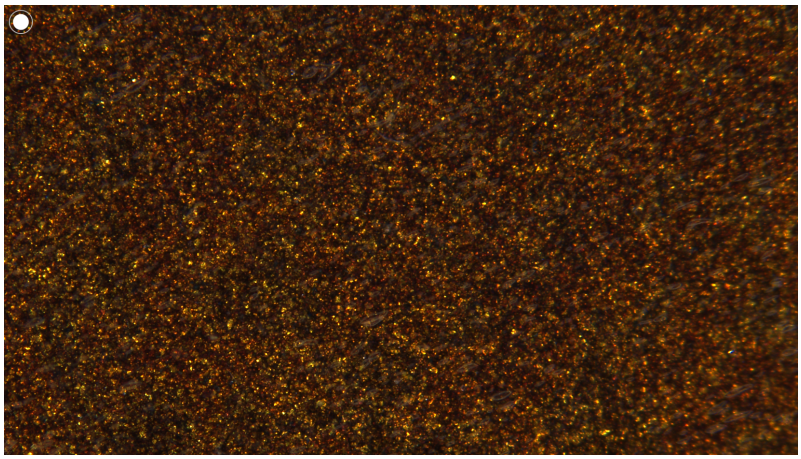

Figure 4.29: Microscopic View: NMC622 Reference Group

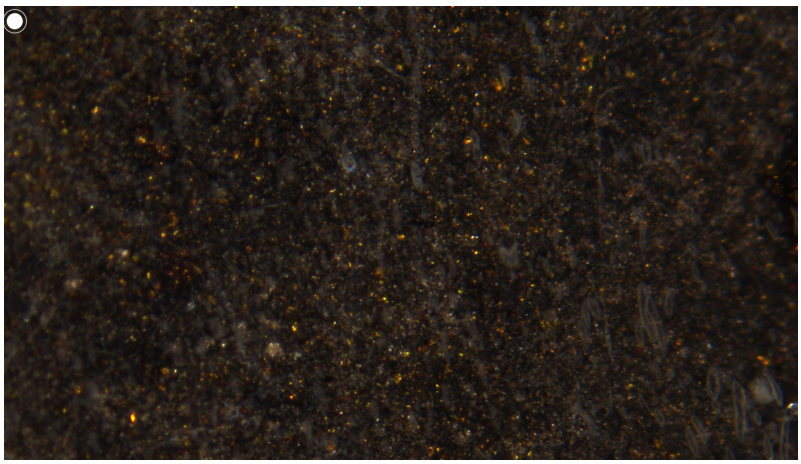

Figure 4.30: Microscopic View: NMC622 Overcharge Group

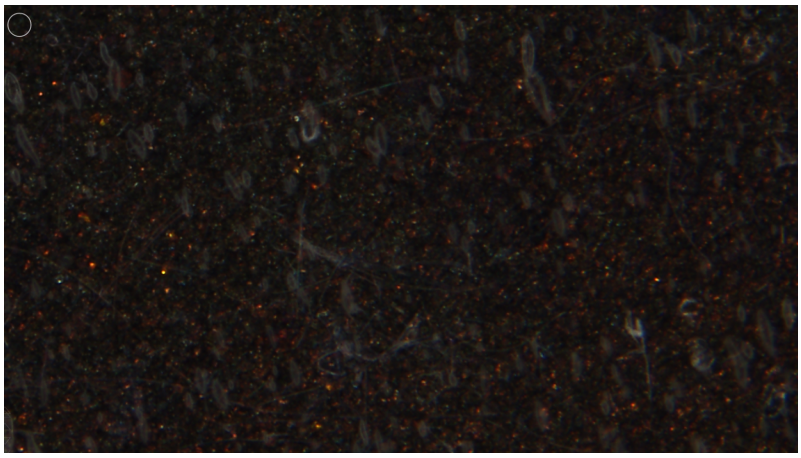

Figure 4.31: Microscopic View: NMC811 Reference Group

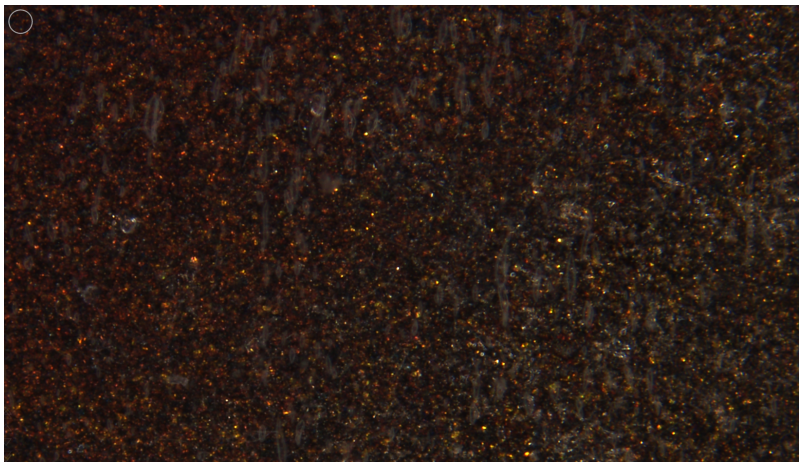

Figure 4.32: Microscopic View: NMC811 Overcharge Group

4.2 Commercial Cell

"This section tested the EIS of commercial batteries after different cycling conditions. The commercial batteries are prismatic cells, primarily composed of NMC811. These tests help verify whether the patterns observed in the commercial batteries align with those found in coin cells made of NMC811. Table 4.1 shows the status of the commercial cells. Due to these batteries undergoing fast charging, it's assumed that all of them have experienced lithium plating. However, due to time constraints, there wasn't enough time for teardowns to confirm the presence of lithium plating definitively.

Cell	SOC	Temp	Charge	Discharge	SOH
A	10-78	45	FC	C/3	32.80
B	10-78	25	FC(derating)	C/3	62.54
C	10-78	25	FC(derating)	C/3	57.43
D	40-78	35	FC	C/3	89.87

Table 4.1: Commercial Cell Battery Status

Due to the varying SOH of the four batteries, to make the Nyquist figure of the commercial batteries more comparable with that of the coin cells, commercial cell D with an SOH of 90% was selected for focused analysis. Figure 4.33 shows the EIS sweep of commercial cell D, with an SOH of 90%. From the fitting line in the figure, it can be seen that the commercial batteries are consistent with the previously mentioned equivalent circuit model 2.2. Additionally, the overall resistance of commercial cells is smaller than that of coin cells, which is largely determined by the structure of the commercial cells. Commercial batteries are typically composed of multiple layers and packages, creating multiple parallel conductive paths that effectively reduce the overall resistance. Furthermore, similar to the pattern observed in Figure 4.3, when the SOC level is at 90%, the Nyquist plot's semicircle is the largest, indicating that the charge transfer resistance is also at its maximum at this SOC level.

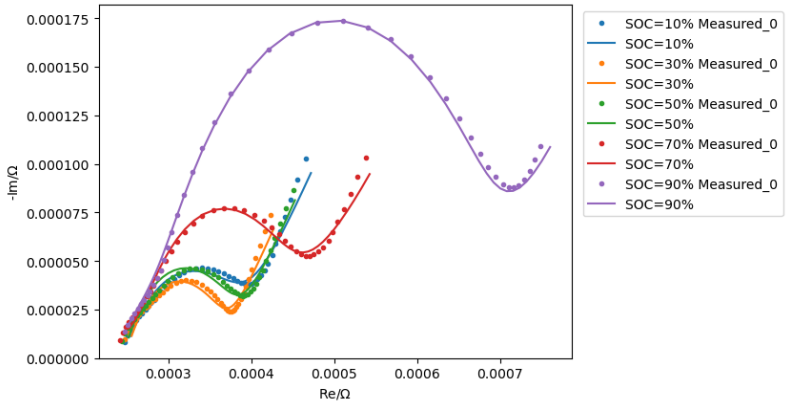

Figure 4.33: EIS sweeps of cell D

Figure 4.34 shows the Nyquist plot of batteries A, B, C, D at SOC 30%, it can be seen that as SOH increases, the battery resistance decreases. This is because the resistance of the battery gradually increases with cycling, and as cycling progresses, the SOH decreases. Figure 4.35 also demonstrates the anode, cathode, and ohmic Resistance in batteries A, B, C, D. It can be observed that as the SOH increases, the anode resistance, cathode resistance, and ohmic resistance all decrease. As the SOH increases, the decrease in cathode and ohmic resistance is reasonable, as both of these resistances typically increase with cycling. However, it is surprising to observe a decrease in anode resistance. It is hypothesized that as the SOH increases, the amount of lithium plating decreases. Lithium plating introduces additional pathways for electron and ion transfer, effectively creating parallel resistances, which may contribute to the observed decrease in anode resistance.

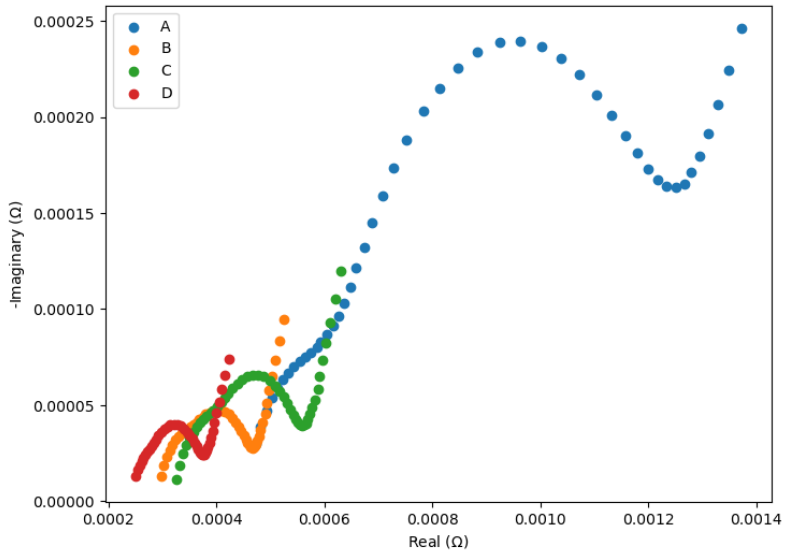

Figure 4.34: Nyquist Plot of Batteries A, B, C, D at SOC30%

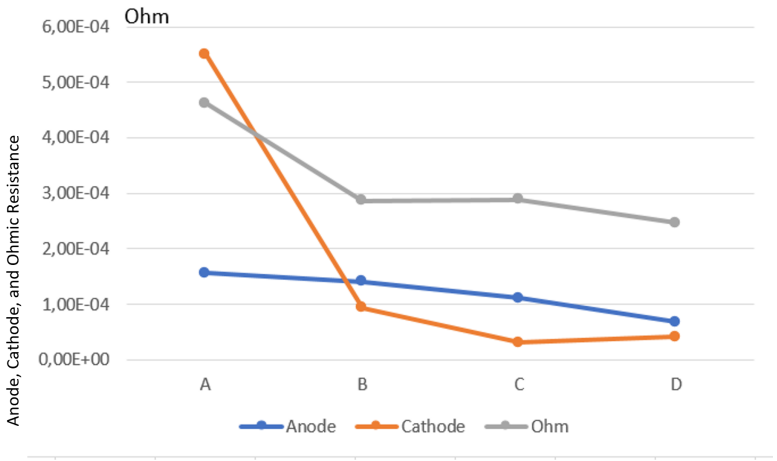

Figure 4.35: Comparative of Batteries A, B, C, D: Anode, Cathode, and Ohmic Resistance

5

Conclusion and Future work

5.1 Conclusion

This report found that both single-sine and multi-sine methods gave similar results, showing that these two measurement methods are equally effective in analyzing electrochemical systems. This is likely because the only difference between them is the frequency spectrum of the injected signals, while other conditions remain consistent, resulting in the capture of similar impedance characteristics. Additionally, equivalent circuit models for coin cells and commercial cells were built using traditional methods, confirming that this approach is reliable for understanding the internal reactions of batteries.

For different materials, the voltage required to induce lithium plating varies, with the voltage limit of NMC622 being lower than that of NMC811. It was verified through EIS, ICA, pulse tests, and capacity retention measurements that, as cycling progresses, the internal resistance of the battery gradually increases. Additionally, NMC811 has a higher initial resistance compared to NMC622, and the resistance fluctuations of NMC811 are more pronounced.

As the battery is overcharged and discharged, lithium plating occurs. In EIS, this causes the Nyquist plot to shift to the right. In ICA, the peak intensity decreases. In pulse tests, resistance increases with cycling, and capacity retention gradually decreases.

5.2 Future work

In the future, Distribution of Relaxation Times (DRT) will continue to be used to convert Nyquist plots into the time domain, helping to observe changes during lithium plating. More half-cell data will be analyzed in pulse tests to investigate the effects on the anode and cathode as lithium plating occurs. Commercial cells will be disassembled to verify the presence of lithium plating and to perform material analysis for further investigation, thereby confirming whether the patterns observed in coin cells are consistent with those in commercial cells. The materials used in coin cells will also be applied to commercial cells to verify if the conclusions are consistent.

Bibliography

[1] Shriram S. Rangarajan, Suvetha Poyyamani Sunddararaj, AVV Sudhakar, Chandan Kumar Shiva, Umashankar Subramaniam, E Randolph Collins, and Tomonobu Senjyu. Lithium-ion batteries—the crux of electric vehicles with opportunities and challenges. *Clean Technologies*, 4(4):908–930, 2022.

[2] Andrew Meintz, Jiucai Zhang, Ram Vijayagopal, Cory Kreutzer, Shabbir Ahmed, Ira Bloom, Andrew Burnham, Richard B Carlson, Fernando Dias, Eric J Dufek, et al. Enabling fast charging–vehicle considerations. *Journal of Power Sources*, 367:216–227, 2017.

[3] Yayuan Liu, Yangying Zhu, and Yi Cui. Challenges and opportunities towards fast-charging battery materials. *Nature Energy*, 4(7):540–550, 2019.

[4] Manuel Weiss, Raffael Ruess, Johannes Kasnatscheew, Yehonatan Levartovsky, Natasha Ronith Levy, Philip Minnmann, Lukas Stolz, Thomas Waldmann, Margret Wohlfahrt-Mehrens, Doron Aurbach, et al. Fast charging of lithium-ion batteries: a review of materials aspects. *Advanced Energy Materials*, 11(33):2101126, 2021.

[5] Anna Tomaszewska, Zhengyu Chu, Xuning Feng, Simon O'kane, Xinhua Liu, Jingyi Chen, Chenzhen Ji, Elizabeth Endler, Ruihe Li, Lishuo Liu, et al. Lithium-ion battery fast charging: A review. *ETransportation*, 1:100011, 2019.

[6] Quentin Hoarau and Etienne Lorang. An assessment of the european regulation on battery recycling for electric vehicles. *Energy Policy*, 162:112770, 2022.

[7] Mathias Petzl, Michael Kasper, and Michael A Danzer. Lithium plating in a commercial lithium-ion battery–a low-temperature aging study. *Journal of power sources*, 275:799–807, 2015.

[8] Xiang Chen, Liangyu Li, Mengmeng Liu, Tao Huang, and Aishui Yu. Detection of lithium plating in lithium-ion batteries by distribution of relaxation times. *Journal of Power Sources*, 496:229867, 2021.

[9] Xianke Lin, Kavian Khosravinia, Xiaosong Hu, Ju Li, and Wei Lu. Lithium plating mechanism, detection, and mitigation in lithium-ion batteries. *Progress in Energy and Combustion Science*, 87:100953, 2021.

[10] Qichao Zhang, Xinzhou Li, Zhichao Du, and Qiangqiang Liao. Aging performance characterization and state-of-health assessment of retired lithium-ion

battery modules. *Journal of Energy Storage*, 40:102743, 2021.

[11] Renjie Wang, Yuanyuan Song, Honglei Xu, Yue Li, and Jie Liu. Life cycle assessment of energy consumption and co2 emission from hev, phev and bev for china in the past, present and future. *Energies*, 15(18):6853, 2022.

[12] Yue Yang, Emenike G Okonkwo, Guoyong Huang, Shengming Xu, Wei Sun, and Yinghe He. On the sustainability of lithium ion battery industry–a review and perspective. *Energy Storage Materials*, 36:186–212, 2021.

[13] Arumugam Manthiram. An outlook on lithium ion battery technology. *ACS central science*, 3(10):1063–1069, 2017.

[14] Linfeng Zheng, Jianguo Zhu, Dylan Dah-Chuan Lu, Guoxiu Wang, and Tingting He. Incremental capacity analysis and differential voltage analysis based state of charge and capacity estimation for lithium-ion batteries. *Energy*, 150:759–769, 2018.

[15] Rui Xiong, Yue Pan, Weixiang Shen, Hailong Li, and Fengchun Sun. Lithium-ion battery aging mechanisms and diagnosis method for automotive applications: Recent advances and perspectives. *Renewable and Sustainable Energy Reviews*, 131:110048, 2020.

[16] Michel Broussely, Ph Biensan, F Bonhomme, Ph Blanchard, S Herreyre, K Nechev, and RJ Staniewicz. Main aging mechanisms in li ion batteries. *Journal of power sources*, 146(1-2):90–96, 2005.

[17] Evelina Wikner. *Lithium ion battery aging: Battery lifetime testing and physics-based modeling for electric vehicle applications*. Chalmers Tekniska Hogskola (Sweden), 2017.

[18] Zachary M Konz, Eric J McShane, and Bryan D McCloskey. Detecting the onset of lithium plating and monitoring fast charging performance with voltage relaxation. *ACS Energy Letters*, 5(6):1750–1757, 2020.

[19] Linda GS Gray and Bernard R Appleman. Eis: electrochemical impedance spectroscopy. *Journal of protective coatings & linings*, 20(2), 2003.

[20] Nina Meddings, Marco Heinrich, Frédéric Overney, Jong-Sook Lee, Vanesa Ruiz, Emilio Napolitano, Steffen Seitz, Gareth Hinds, Rinaldo Raccichini, Miran Gaberšček, et al. Application of electrochemical impedance spectroscopy to commercial li-ion cells: A review. *Journal of Power Sources*, 480:228742, 2020.

[21] Juan José Giner-Sanz, EM Ortega, and Valentín Pérez-Herranz. Application of a montecarlo based quantitative kramers-kronig test for linearity assessment of eis measurements. *Electrochimica Acta*, 209:254–268, 2016.

[22] Chen You, Mohammed Ahmed Zabara, Mark E Orazem, and Burak Ulgut. Application of the kramers–kronig relations to multi-sine electrochemical impedance measurements. *Journal of the Electrochemical Society*, 167(2):020515, 2020.

[23] Andreas Straßer, Alexander Adam, and Jiahao Li. In operando detection of lithium plating via electrochemical impedance spectroscopy for automotive batteries. *Journal of Power Sources*, 580:233366, 2023.

[24] EL-CELL. Pat-cell, 2024. https://www.el-cell.com/products/test-cells/standard-test-cells/pat-cell/, Accessed: 2024-05-29.

DEPARTMENT OF SOME SUBJECT OR TECHNOLOGY
CHALMERS UNIVERSITY OF TECHNOLOGY
Gothenburg, Sweden
www.chalmers.se

CHALMERS
UNIVERSITY OF TECHNOLOGY